Interference Graph Estimation for Full-Duplex mmWave Backhauling: A Power Control Approach

Haorui Li, Daqian Ding, and Yibo Pi
Shanghai Jiao Tong University, Shanghai, China

***Abstract*—Traditional wisdom for network resource management is to allocate separate frequency-time resources for measurement and data transmission tasks. As a result, the two types of tasks have to compete for resources, and a heavy measurement task inevitably reduces available resources for data transmission. This prevents interference graph estimation (IGE), a heavy yet important measurement task, from being widely used in practice. To resolve this issue, we propose to use power as a new dimension for interference measurement in full-duplex mmWave backhaul networks, such that no extra frequency-time resources are needed for measurement. Our core insight is to consider the mmWave network as a linear system, where the received powers of a node can be expressed as the product of the powers of transmitters and the equivalent channel gains from the transmitters to the node. By controlling the powers of transmitters, we can find unique solutions for the equivalent channel gains, which will then be used to estimate interference. To accomplish resource allocation and IGE simultaneously, we jointly optimize resource allocation and IGE with power control. Extensive simulations show that significant links in the interference graph can be accurately estimated with less than 3% increase in power consumption, independent of the time synchronization and carrier frequency offset (CFO) estimation errors between nodes.**

***Index Terms*—mmWave backhauling, interference graph estimation, resource allocation**

I. Introduction

Network densification is a key mechanism to increase spectrum reuse such that the network capacity can be greatly boosted for future explosive growth of user demand. However, dense deployment of small cells is costly with a fiber backhaul [1]. For fast and cost-effective deployment of dense small cells, millimeter-wave (mmWave) backhauling is proposed as a promising backhaul alternative. In mmWave communications, to combat large path loss in high-frequency bands, the transmitters generally employ beamforming techniques to direct their beams towards the receivers, resulting in less interference between links. Despite that, under dense deployment, mmWave networks are shown to still operate in the interference-limited regime: the network capacity is significantly affected by the interference among nodes [2]. Further, the inter-link interference is exacerbated when full-duplex capabilities are used to improve the network capacity by allowing more concurrent transmissions. It is thus critical to effectively manage interference for resource allocation in full-duplex mmWave backhaul networks.

In dense mmWave networks, interference-aware resource allocation has been extensively studied, where interference is depicted in various forms. The simplest form is a conflict graph (or contention graph) dictating if two links can be active at the same time [3], [4]. To construct a conflict graph, we typically need to estimate the interference between each pair of links. A network with n links includes $O(n^2)$ pairs of links to be measured, incurring heavy measurement overhead. It is possible to reduce the measurement overhead by measuring only a subset of links and inferring the rest using matrix completion [5] or graph embedding techniques [6]. However, these techniques leverage node or link similarities to predict interference distribution, with no accuracy guarantee at the link level. More importantly, conflict graphs depict the binary relations between links, which cannot capture the additive nature of interference.

The second form to characterize interference in mmWave communications is modelling, which can be used to estimate the magnitude of interference and to capture its additive nature. Modelling the channel and antenna patterns of one mmWave link requires choosing proper model parameters based on the propagation environment and there exist a variety of choices. A mmWave channel could consist of either a single LOS component, purely scattering components, or a mix of both the LOS and scattering components [7], [8]. Each component could further experience different degrees of path loss and fading [9], [10]. Both the complexities and errors in modelling the channel and antenna patterns make it impractical to estimate the interference accurately. This leads to poor resource allocation decisions and, consequently, degraded network performance.

More recently, considering the complexities in both interference modelling and measurements, machine learning techniques have been used to learn a direct mapping from network information to resource allocation decisions without directly estimating the interference. In [11], a deep learning approach is proposed to use the geographic locations of nodes as input and learn link scheduling decisions from a large scale of network layouts to achieve the maximum sum rate in device-to-device networks. Further improvement using graph embedding and deep neural networks reduces the scale of training data from hundreds of thousands to hundreds of network layouts [12]. These data-driven techniques require knowing the static attributes of nodes (e.g. locations), not adaptive to dynamic network conditions, e.g., fading.

Compared to the approaches above, the most practical one is introduced in 4G LTE-A to measure the interference between base stations (BSs) and user equipments (UEs) using CSI-

979-8-3503-1090-0/23/$31.00 © 2023 IEEE

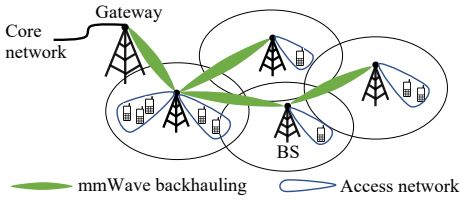

Fig. 1. Multi-hop mmWave backhauling

IM reference signals. Specifically, when the serving BS of an UE sends no signal on a CSI-IM resource element (RE), the received signal strength of the UE is then the interference from other BSs on that RE. For scheduling purposes, interference has to be measured separately for each interfering BS, requiring operations that tell UEs which REs to measure and which REs to be used for reporting back measurements. This incurs heavy measurement overheads when the number of interfering BSs is large, especially in dense networks. More importantly, this process requires nanosecond-scale synchronization between BSs and accurate estimation of carrier frequency offsets (CFOs) between UEs and their interfering BSs, where strict time synchronization is difficult in a fiber backhaul [13] and becomes even harder in a multi-hop wireless backhaul [14].

Motivated by these challenges, we want to 1) efficiently estimate the interference graph, depicting the inter-link interference, for full-duplex mmWave backhaul networks under imperfect time synchronization and carrier frequency offset (CFO) estimation, and 2) use it to improve the efficiency of resource allocation. We propose to use power as a new dimension for interference graph estimation (IGE) such that no extra frequency-time resources need to be consumed. Our core insight is that the received power of a node can be expressed as a linear combination of channel gains and the powers of transmitters. In a time-slotted network, manipulating the powers of transmitters enables each node to have different received powers across time slots, i.e., a group of linear equations. Channel gains can have a unique solution if the powers of transmitters form a full-rank matrix.

In summary, our contributions in this paper are as follows.

- We show that the mmWave network can be considered as a linear system and propose to estimate the interference graph by manipulating the transmit powers of nodes, robust to time synchronization and CFO estimation errors.
- We formulate the problem of joint resource allocation and IGE, such that IGE can be done simultaneously with resource allocation without consuming extra frequency-time resources.
- We evaluate our approach with extensive simulations under various network settings and show that our approach can accomplish resource allocation and IGE simultaneously with minimal overhead on power consumption.

II. System Model

A. Millimeter-Wave Backhauling

We consider a multi-hop mmWave backhaul network with K BSs, one of which serves as a gateway to the core network, as shown in Figure 1. Each BS is equipped with a full-duplex radio such that it can transmit data to one node and receive data from another node simultaneously. All BSs are assumed to be time-synchronized and scheduled to transmit and receive data at specified time slots. The scheduling decision is made at the gateway in a centralized way, which requires each BS to report local measurements of the channel information back to the gateway. After a scheduling plan is made, it is disseminated from the gateway to all BSs. Both the data collection and dissemination for network management purposes are done through the backhaul network using the control channel. Each BS modulates the transmitted symbols with orthogonal frequency division multiplexing (OFDM) and uses all N_c subcarriers for each transmission. Concurrent transmissions in the same time slot may interfere with each other.

We consider the CFO and timing offset (TO) between BSs. Since BSs are not mobile, the Doppler frequency shift is negligible and CFO is mainly caused by the oscillator mismatch in frequency. The TO arises from the synchronization errors among BSs as well as the difference in the propagation delays when considering the signals from multiple transmitters to the same receiver. We assume that no cooperative transmission is used and that each receiver is assumed to receive data from a single transmitter. For demodulation, each receiver only estimates the CFO of the transmitter and will not compensate the CFOs of other transmitters.

B. Channel Model

Let (k,z) be the directional link from BS k to z, and $\mathcal{E}$ be the set of all directional links. For simplicity, each BS is assumed to have an M-antenna array and the channel from BS k to z is denoted as $\mathbf{H}_{(k,z)} \in \mathbb{C}^{M\times M}$. When BS k is transmitting to BS z, the transmit and receive beamforming vectors of BSs k and z are $\widetilde{\boldsymbol{\gamma}}_{(k,z)} \in \mathbb{C}^{M\times 1}$ and $\widetilde{\boldsymbol{\omega}}_{(k,z)} \in \mathbb{C}^{M\times 1}$, respectively. Since BSs are typically deployed at high places with fixed locations, the channel coherence time between BSs is relatively stable [15], and $\mathbf{H}_{(k,z)}$ is assumed to be a slow time-varying fading channel. We denote the residual CFO of BS k with respect to BS z as $\phi_{(k,z)}$, normalized to the subcarrier spacing with a range between -0.5 and 0.5, and the integer-valued TO of link (k,z) as $\mu_{(k,z)}$. Let $x_{(k,z)}[i]$ and $y_{(k,z)}[i]$ be the i-th discrete transmitted and received samples for the link (k,z), respectively. The i-th received sample for link (k,z) can be expressed as

$$y_{(k,z)}[i] = \widetilde{\boldsymbol{\omega}}_{(k,z)}^T \left(\sum_{(l,d)\in\mathcal{E}} e^{j2\pi i\phi_{(l,z)}} \mathbf{H}_{(l,z)} \widetilde{\boldsymbol{\gamma}}_{(l,d)} x_{(l,d)}[i-\mu_{(l,d)}] + \boldsymbol{v}[i] \right)$$

where $\mathcal{E}$ is the set of all links and $\boldsymbol{v}[i] \sim \mathcal{CN}(\mathbf{0},\sigma^2\mathbf{I})$ is the noise variance at each antenna of the receiving BS. Let $h^{\text{eq}}_{(l,d),(k,z)} = \widetilde{\boldsymbol{\omega}}_{(k,z)}^T \mathbf{H}_{(l,z)} \widetilde{\boldsymbol{\gamma}}_{(l,d)}$. We can rewrite the equation above as

$$y_{(k,z)}[i] = \sum_{(l,d)\in\mathcal{E}} e^{j2\pi i\phi_{(l,z)}} h^{\text{eq}}_{(l,d),(k,z)} x_{(l,d)}[i-\mu_{(l,d)}] + \widetilde{v}[i],$$

where $\widetilde{v}[i] = \widetilde{\boldsymbol{\omega}}_{(k,z)}^T \boldsymbol{v}[i]$. The time-domain sample $x_{(l,d)}[i]$ is the inverse discrete Fourier transform (IDFT) of the modulated symbols, $\{X_{(l,d)}[r]\}_{r=0}^{N_c-1}$, i.e.,

$$x_{(k,z)}[i] = \frac{1}{\sqrt{N}} \sum_{l=0}^{N_c-1} X_{(k,z)}[l] e^{j2\pi il/N_c}, 0 \le n \le N_c+N_g-1,$$

where $X_{(k,z)}[l]$ is the modulated symbol on the l-th subcarrier transmitted from BS k to z, and N_g is the length of the cyclic prefix (CP).

C. Interference Model

In the mmWave network, each node employs the beamforming techniques to generate a radiation pattern with a main beam and multiple side lobes. Due to hardware constraints, the mmWave nodes could have limited codebook size for beamforming and irregular radiation patterns [16], which makes interference nulling difficult. We thus consider the interference from both the main beam and the side lobes of transmitters. In mmWave communications, interference depends on the directions of both transmission and reception. Suppose that nodes s and k are transmitting to nodes l and z, respectively. The interference from link (s,l) to link (k,z), denoted as $g_{(s,l),(k,z)}$, can be expressed as a product of the transmission gain at node s, the channel gain of the interference link from node s to z, and the reception gain at node z with beamforming towards node k, denoted as $g^t_{(s,l),(k,z)}$, $g^c_{(s,l),(k,z)}$, and $g^r_{(s,l),(k,z)}$, respectively. Let $p^{tx}_{(k,z)}$ be the transmit power of node k to node z, and $p^{rx}_{(k,z)}$ be the received power of node z from node k. We can express the received power of node z as

$$p^{rx}_{(k,z)} = \sum_{(s,l)\in\mathcal{E}} \underbrace{g^t_{(s,l),(k,z)} g^c_{(s,l),(k,z)} g^r_{(s,l),(k,z)}}_{g_{(s,l),(k,z)}} p^{tx}_{(s,l)} + BN_0,$$

where B is the mmWave bandwidth and N_0 is the noise power spectral density. Suppose that node k is transmitting to node z, we can express the signal-to-interference-plus-noise ratio (SINR) at node z as

$$\text{SINR}_{(k,z)} = \frac{g_{(k,z),(k,z)} p^{tx}_{(k,z)}}{p^{rx}_{(k,z)} - g_{(k,z),(k,z)} p^{tx}_{(k,z)}},$$

where $g_{(s,l),(k,z)} = \left| h^{\text{eq}}_{(l,d),(k,z)} \right|^2$.

III. Interference Graph Estimation: A Power Control Approach

A. Estimating Interference Graph with Power Control

Lemma 1. *In analog beamforming mmWave networks, if $\mathbb{E}[|X_{(s,d)}[i]|^2] = \mathbb{E}[|X_{(s,d)}[j]|^2]$ and $\mathbb{E}[X_{(s,d)}[i]] = 0$ for all i's and (s,d)'s, the expected receive power of node z with beamforming towards node k, i.e., $\mathbb{E}[|y_{(k,z)}[i]|^2]$, is a linear combination of the equivalent channel gains and the expected transmit powers of nodes over links, independent of TOs and CFOs, i.e.,*

$$\mathbb{E}[|y_{(k,z)}[i]|^2] = \sum_{(l,d)\in\mathcal{E}} g_{(l,d),(k,z)} \mathbb{E}[|x_{(l,d)}[i]|^2] + W, \quad (1)$$

where $g_{(l,d),(k,z)}$ is the equivalent channel gain between links (l,d) and (k,z).

Proof: Please refer to Appendix A. ∎

Let s_i and r_i be the senders and receiver of the i-th directional link, respectively, and $p^{tx}_{(s_i,r_i)}[t]$ and $p^{rx}_{(s_i,r_i)}[t]$ be the transmit and receive powers of nodes s_i and r_i at time t.

Theorem 1. *The equivalent channel gains between links can be estimated by controlling the transmit powers of senders of different links over time such that*

$$rank(\mathbf{P}^{tx}) = |\mathcal{E}|, \quad (2)$$

where $\mathbf{P}^{tx} = \left[\mathbf{p}^{tx}_{(s_1,r_1)}, \ldots, \mathbf{p}^{tx}_{(s_{|\mathcal{E}|},r_{|\mathcal{E}|})}\right]$ and $\mathbf{p}^{tx}_{(s_i,r_i)} = [p^{tx}_{(s_i,r_i)}[j], \ldots, p^{tx}_{(s_i,r_i)}[j+n-1]]^T$ includes the transmit powers of the sender at link (s_i,r_i) from time j to $j+n-1$.

Proof: Let $\boldsymbol{p}^{rx}_{(k,z)} = \left[p^{rx}_{(k,z)}[j], \ldots, p^{rx}_{(k,z)}[j+n-1]\right]^T$ be the receive powers of node z with beamforming towards node k at different times, and $\boldsymbol{w} = [W, \ldots, W]^T$ be the vector of noise power. According to Eq. (1), we can have

$$\boldsymbol{p}^{rx}_{(k,z)} = \mathbf{P}^{tx} \mathbf{g}_{(k,z)} + \boldsymbol{w}, \quad (3)$$

where $\mathbf{g}_{(k,z)} = [g_{(s_1,e_1),(k,z)}, \ldots, g_{(s_{|\mathcal{E}|},e_{|\mathcal{E}|}),(k,z)}]^T$, $(s_i,e_i) \in \mathcal{E}$. Since $\mathbf{P}^{tx} \in \mathbb{R}^{n\times|\mathcal{E}|}$ and $n \ge |\mathcal{E}|$, $\mathbf{g}_{(k,z)}$ has a unique solution if $rank(\mathbf{P}^{tx}) = |\mathcal{E}|$.

From Theorem 1, we know that the channel gains can be estimated if the actual transmit powers can approximate the expected transmit powers and form a full-rank matrix. ∎

IV. Joint Optimization for Interference Graph Estimation and Resource Allocation

A. Problem Formulation

We assume that each node has a single path to the gateway, which is determined by the routing algorithm. Based on the buffer status reports of UEs, we can infer the traffic demand for each link. Our goal is to maximize the energy efficiency of the mmWave backhaul network in satisfying the traffic demand within the required number of time slots. Since the traffic demand for each link is fixed, the joint optimization problem can be formulated as follows.

$$(\mathcal{P}1) \min_{\mathbf{P},\boldsymbol{\delta}} \sum_{k\in\mathcal{K}} \sum_{(i,j)\in\mathcal{E}} p^{tx}_{(i,j)}[k]\tau$$

$$\text{s.t.} \quad (C_1) \sum\nolimits_{j\in\mathcal{K}} \delta_{(j,i)}[k] \le 1, \forall i \in \mathcal{K},$$
$$(C_2) \sum\nolimits_{j\in\mathcal{K}} \delta_{(i,j)}[k] \le 1, \forall j \in \mathcal{K},$$
$$(C_3)\ \delta_{(i,j)}[k] \in \{0,1\}, \forall (i,j) \in \mathcal{E},$$
$$(C_4) \sum_{k=1}^{M} \delta_{(i,j)}[k] \ge \left\lceil \frac{D_{(i,j)}}{R_{(i,j)}\tau} \right\rceil, \forall (i,j) \in \mathcal{E},$$
$$(C_5)\ \text{SINR}_{(i,j)} \ge \gamma_{(i,j)} \delta_{(i,j)}[k], \forall (i,j) \in \mathcal{E},$$
$$(C_{6.1})\ p^{tx}_{(i,j)}[k] \ge \delta_{(i,j)}[k] P_{min}, \forall (i,j) \in \mathcal{E},$$
$$(C_{6.2})\ p^{tx}_{(i,j)}[k] \le \delta_{(i,j)}[k] P_{max}, \forall (i,j) \in \mathcal{E},$$
$$(C_7)\ rank(\mathbf{P}^{tx}) = |\mathcal{E}|,$$

where τ is the time slot length, $\delta_{(i,j)}[k]$ indicates if node i is sending to node j at k-th time slot, $D_{(i,j)}$ is the traffic demand for link (i,j), and $R_{(i,j)}$ is the transmission rate under the selected modulation and coding scheme (MCS), $\gamma_{(i,j)}$ is the required SINR of link (i,j) that can support the transmission rate $R_{(i,j)}$, $\mathcal{K}$ is the set of indices for time slots, P_{max} and P_{min} are the boundary powers.

B. Proposed Solution

Since τ is fixed, we want to minimize the total transmit power. To solve this rank-constrained mixed-integer nonlinear programming (MINLP), we divide $\mathcal{P}1$ into two subproblems: a MINLP without the rank constraint, i.e.,

$$(\mathcal{P}2)\ \min_{\boldsymbol{P},\boldsymbol{\delta}} \sum_{i\in\mathcal{K}}\sum_{(i,j)\in\mathcal{E}} p^{tx}_{(i,j)}[k] \quad \text{s.t. } C_1\text{-}C_6,$$

and a rank-constrained linear programming problem, i.e.,

$$(\mathcal{P}3)\ \min_{\boldsymbol{P}} \sum_{i\in\mathcal{K}}\sum_{(i,j)\in\mathcal{E}} p^{tx}_{(i,j)}[k] \quad \text{s.t. } C_5\text{-}C_7,$$

where $\mathcal{P}2$ first determines the on/off states of links in each time slot, indicated by $\boldsymbol{\delta}$, and then $\mathcal{P}3$ bases on $\boldsymbol{\delta}$ to obtain the power allocation $\boldsymbol{P}$ that satisfies the rank constraint. $\mathcal{P}3$ is different from $\mathcal{P}1$ in that as $\boldsymbol{\delta}$ is given in $\mathcal{P}3$, its variable list does not include $\boldsymbol{\delta}$, making it not a mixed-integer problem. We solve each subproblem as follows.

C. Solution to $\mathcal{P}2$

1) Continuous Relaxation: As mentioned, $\mathcal{P}2$ is a nonconvex MINLP. We first relax the binary variables $\delta_{(i,j)}[k]$'s into continuous that $\delta_{(i,j)}[k] \in [0,1]$. As a result, the problem becomes a nonconvex nonlinear problem. After the problem is solved, we want to convert relaxed continuous $X_{(i,j)}[k]$'s back to binary and thus introduce a penalty term in the objective function to penalize $\delta_{(i,j)}[k]$'s for deviating from 0 or 1. The penalty term is $f(\boldsymbol{\delta}) = g_1(\boldsymbol{\delta}) + g_2(\boldsymbol{\delta})$, where $g_1(\boldsymbol{\delta}) = \sum_{k\in\mathcal{K}}\sum_{(i,j)\in\mathcal{E}} \delta_{(i,j)}[k]$ and $g_2(\boldsymbol{\delta}) = -\sum_{k\in\mathcal{K}}\sum_{(i,j)\in\mathcal{E}}(\delta_{(i,j)}[k])^2$. Suppose $\boldsymbol{\delta}^{(t-1)}$ is a feasible solution at the $(t-1)$-th iteration. $g_2(\boldsymbol{\delta})$ can be linearized by its first-order Taylor approximation near $\boldsymbol{\delta}^{(t-1)}$ as

$$g_2(\boldsymbol{\delta}) \le \tilde{g_2}(\boldsymbol{\delta}) \triangleq g_2(\boldsymbol{\delta}^{(t-1)}) + \nabla g_2^T(\boldsymbol{\delta}^{(t-1)})(\boldsymbol{\delta} - \boldsymbol{\delta}^{(t-1)}).$$

2) Convex Relaxation: $\mathcal{P}2$ is nonconvex due to constraint C_5. A popular way of solving nonconvex problems is successive convex approximation (SCA), which relaxes the nonconvex problem into a convex one and iteratively solve the convex problem until convergence. To relax constraint C_5, we rewrite it into two constraints, i.e.,

$$(C_{5.1})\ s_{(i,j)}[k] = BN_0 + \sum_{(l,d)\in\mathcal{E}\setminus(i,j)} g_{(l,d),(i,j)} p^{tx}_{(l,d)}[k], \quad (4)$$

and

$$(C_{5.2})\ \frac{p^{tx}_{(i,j)}[k]}{\gamma_{(i,j)}} g_{(i,j),(i,j)} \ge \delta_{(i,j)}[k] s_{(i,j)}[k]. \quad (5)$$

Following the principle of SCA, we need to find a convex surrogate function for the nonconvex term in $C_{5.2}$ as

$$\delta_{(i,j)}[k]s_{(i,j)}[k] \le \frac{\phi_{(i,j)}[k]}{2}(\delta_{(i,j)}[k])^2 + \frac{(s_{(i,j)}[k])^2}{2\phi_{(i,j)}[k]} \quad (6)$$

for any constant $\phi_{(i,j)}[k] > 0$, where the equality holds when $\phi_{(i,j)}[k] = s_{(i,j)}[k]/\delta_{(i,j)}[k]$. Then, constraint $C_{5.2}$ becomes

$$(C_{5.3})\ \frac{g_{(i,j),(i,j)}}{\gamma_{(i,j)}} p^{tx}_{(i,j)}[k] \ge \frac{\phi_{(i,j)}[k]}{2}(\delta_{(i,j)}[k])^2 + \frac{(s_{(i,j)}[k])^2}{2\phi_{(i,j)}[k]},$$

which is a convex constraint.

Let $\boldsymbol{S}$ be the matrix for $s_{(i,j)}[k]$'s. At the t-th iteration, $\mathcal{P}2$-1 can then be relaxed as

$$(\mathcal{P}2\text{-}1)\ \min_{\boldsymbol{P},\boldsymbol{\delta},\boldsymbol{S}} \sum_{i\in\mathcal{C}}\sum_{k\in\mathcal{K}} p^{tx}_{(i,j)}[k] + \lambda g_1(\boldsymbol{\delta}) + \lambda \tilde{g}_2(\boldsymbol{\delta})$$
$$\text{s.t. } C_1, C_2, C_4, C_{5.1}, C_{5.3}, C_6,$$
$$\delta_{(i,j)}[k] \in [0,1]$$

which is a second-order cone programming (SOCP) problem. The solution to $\mathcal{P}2$ can be obtained by iteratively solving $\mathcal{P}2$-1 until convergence.

D. Solution to $\mathcal{P}3$

When $\boldsymbol{\delta}$ is given, constraint C_5 becomes linear and $\mathcal{P}3$ is a rank-constrained linear programming problem. As shown in [17], rank constraints are discontinuous and nonconvex, which needs to be gradually approximated with a sequence of semidefinite programming (SDP) problems. To approximate constraint C_7, we reformulate it with the rank constraints of two semidenifinite matrices. Specifically, we have $rank(\boldsymbol{P}) = |\mathcal{E}|$ if and only if there exists a $\boldsymbol{Z} \in \mathbb{S}^n$ such that

$$rank(\boldsymbol{Z}) = |\mathcal{E}|,$$

and

$$rank\,(\boldsymbol{U}) \leqslant |\mathcal{E}|,\ \boldsymbol{U} = \begin{bmatrix} \boldsymbol{I}_{|\mathcal{E}|} & \boldsymbol{P}^T \\ \boldsymbol{P} & \boldsymbol{Z} \end{bmatrix},$$

where $\mathbb{S}^n$ is the set of symmetric $n \times n$ matrices. Based on the theorem in [17], we have that when $e = 0$ and $\boldsymbol{U}$ is a positive semidefinite matrix, $rank(\boldsymbol{Z}) = |\mathcal{E}|$ and $rank(\boldsymbol{U}) \leqslant |\mathcal{E}|$ are equivalent to

$$V_p^T \boldsymbol{Z} V_p > 0, \text{ and } e\boldsymbol{I}_n - \boldsymbol{W}^T \boldsymbol{U} \boldsymbol{W} \succeq 0$$

where the vector $V_p \in \mathbb{R}^{n\times 1}$ is the eigenvector corresponding to the $n - |\mathcal{E}| + 1$ smallest eigenvalue of $\boldsymbol{Z}$, and the matrices $\boldsymbol{W} \in \mathbb{R}^{(n+|\mathcal{E}|)\times n}$ are the eigenvectors corresponding to the n smallest eigenvalues of $\boldsymbol{U}$.

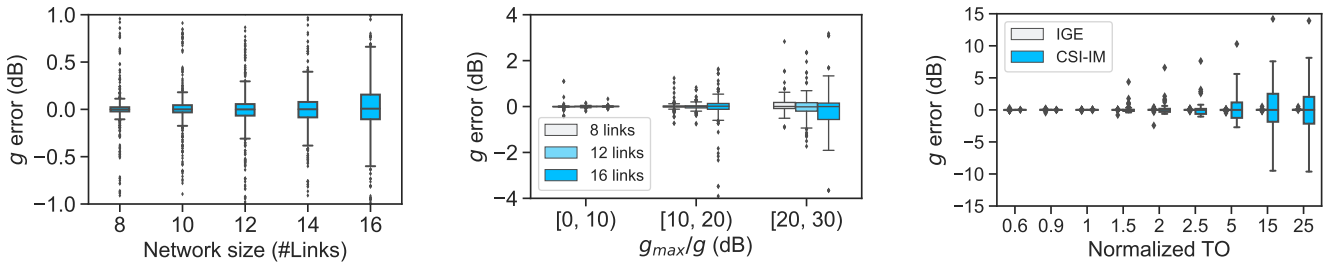

(a) Estimation error vs. network size (b) Distribution of estimation errors (c) Robustness to TO

Fig. 2. Accuracy of interference graph estimation

TABLE I
SIMULATION PARAMETERS

#Antenna per BS	100	BS distance	15-200m
Time slot length	1ms	Tx power range	800-1200mW
Carrier frequency f_c	28GHz	Noise spectrum	-174dBm/Hz
Total bandwidth	250MHz	BS density	$\geq$ 500BSs/km^2

Replacing the rank constraints with the SDP ones, we can solve $\mathcal{P}3$ by iteratively solving the following problem:

$$\min_{\boldsymbol{P}^{(t)},\boldsymbol{Z}^{(t)},e^{(t)}} \sum_{i\in\mathcal{C}}\sum_{k\in\mathcal{K}} p_{(i,j)}^{(t)}[k] + w^{(t)}e^{(t)} \tag{7a}$$

$$\text{s.t.} \quad \left(V_p^{(t-1)}\right)^T \boldsymbol{Z}^{(t)} V_p^{(t-1)} > 0 \tag{7b}$$

$$e^{(t)}\boldsymbol{I}_n - \left(\boldsymbol{W}^{(t-1)}\right)^T \boldsymbol{U}^{(t)}\boldsymbol{W}^{(t-1)} \succeq 0 \tag{7c}$$

$$0 \leq e^{(t)} \leq e^{(t-1)} \tag{7d}$$

$$C_5, C_6, C_7 \tag{7e}$$

$$\boldsymbol{Z}^{(t)} \succeq \boldsymbol{0}, \boldsymbol{U}^{(t)} \succeq \boldsymbol{0} \tag{7f}$$

where $p_{(i,j)}^{(t)}[k]$ is $p_{(i,j)}^{tx}[k]$ at the t-th iteration, $\boldsymbol{W}^{(t-1)}$ includes the eigenvectors of $\boldsymbol{U}^{(t-1)}$, and $w^{(t)}$ is a weighting factor increasing with the iteration count t. The starting point at the 0-th iteration can be obtained by solving Eq. (7) without constraints (7b)-(7d) as in [17]. At the first iteration where $t = 0$, $e^{(0)}$ is the n-th smallest eigenvalue of $\boldsymbol{U}^{(0)}$.

V. PERFORMANCE EVALUATION

The performance of our proposed joint optimization is evaluated via simulations. The simulation parameters are chosen to simulate a typical 5G mmWave backhaul network, as listed in Table I. Our experiment simulates a small cluster of dense BSs, where BSs are randomly located in a 0.01km^2 square field with density more than 500 BSs/km^2. The mmWave channel model consists of a LOS component and a scattering component with independent and identically distributed entries as in [8]. Each BS has access to a uniform linear array (ULA) with 100 antennas. The angle-of-arrival (AoA) at each BS is the direction from which the strongest signal strength is detected, which are used to estimate the transmit and receive beamforming vectors of BSs. The MCSs are randomly selected for UEs and UEs are assumed to have heavy demands, which require at least 80% of total time slots.

Channel gain estimation. Let the actual and estimated equivalent channel gains between links (s,l) and (k,z) be denoted as $g_{(s,l),(k,z)}$ and $\hat{g}_{(s,l),(k,z)}$, respectively. We measure the error of channel gain estimation as $10\log_{10}\left(\hat{g}_{(s,l),(k,z)}/g_{(s,l),(k,z)}\right)$ in dB, which is equal to zero when the actual and estimated channel gains are equal and increases in its absolute value as the measured one deviates away from the actual one. Fig. 2(a) shows the boxplot of the estimation errors using our approach under different network sizes, where the network size is measured by the number of links in the backhaul network. We can see that our approach achieves small estimation errors below 1dB for almost all the links, with half of the estimation errors less than 0.2dB. The estimation errors slightly increase with the network size due to increasing number of concurrent transmissions, which causes more severe interference. The increasing number of interferers weakens the linearity between the transmit and received powers of nodes and thus results in larger estimation errors.

We also find that small channel gains are prone to large estimation errors. Fig. 2(b) shows the estimation errors with respect to the channel gain ratios, where g_{max} is the maximum channel gain in a network layout. We can see that smaller channel gains tend to have larger estimation errors. Luckily, links with small equivalent channel gains have weak interference to each other, mitigating the impact of relatively large estimation errors. Lastly, we want to compare our approach with CSI-IM reference signals. Fig. 2(c) shows the estimation errors under different TOs, where the TO is normalized with respect to CP. We find that the CSI-IM achieves very small estimation errors when TO is less than CP, as expected. However, as TO exceeds CP, the estimation errors continue to increase until TO reaches 15 (CP takes 7% of OFDM symbol time), where the TO is equal to a OFDM symbol time in our experiment. In contrast, our approach is robust to TO and achieves very small estimation errors under all TOs.

Power overhead. Our approach uses power as a new dimension for interference measurement and thus may have extra power overhead. We compare our approach with the pure resource allocation scheme not considering IGE (i.e., $\mathcal{P}2$) in terms of power consumption. Let P_1 and P_0 denote the power consumption in our approach and the pure power resource allocation scheme, respectively. We define *power overhead* as $(P_1 - P_0)/P_0$. Fig. 3 shows the boxplot for power

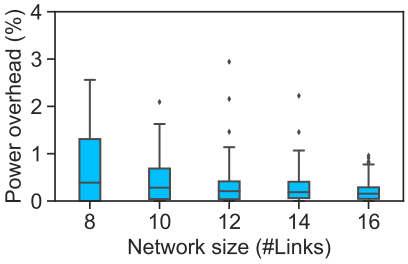

Fig. 3. Power overhead

overheads under different network sizes, where 100 random layouts are used for each network size. The positive power overheads indicate that our approach estimates the interference graph at the cost of power consumption. Fortunately, even the worst power overhead is below 3% and the average is below 1%. Further, the power overhead in general decreases as the network size increases, because the extra power consumption needed for power control increases slower than the total power consumption of the network.

VI. Conclusion

In this paper, we proposed to use power as a new dimension for interference graph estimation, such that it can be done simultaneously with resource allocation, with no extra frequency-time resources needed. To this end, we proved that the mmWave backhaul network can be considered as a linear system and that the interference graph can be measured with power control. Our joint optimization of resource allocation and IGE outperforms the reference signals in channel gain estimation for being more robust to timing and carrier frequency offsets. Moreover, the overhead of our approach was showed to be very small by experiments. As future work, we will apply the joint framework to other wireless networks.

VII. Acknowledgement

We appreciate the constructive feedback from the anonymous reviewers. This work was supported by the National Natural Science Foundation of China under Grant 62201346.

Appendix A
Proof of Lemma 1

Since $\boldsymbol{v}[i] \sim \mathcal{CN}(\mathbf{0}, \sigma_v^2\mathbf{I})$, $\mathbb{E}[\widetilde{v}[i]] = \mathbb{E}[\widetilde{\boldsymbol{\omega}}_{(k,z)}^T \boldsymbol{v}[i]] = 0$ and $\mathbb{E}\left[|\widetilde{v}[i]|^2\right] = \widetilde{\boldsymbol{\omega}}_{(k,z)}^T \mathbb{E}\left[\boldsymbol{v}[i]\boldsymbol{v}[i]^H\right] \widetilde{\boldsymbol{\omega}}_{(k,z)}^* = \sigma_v^2$. Let $F_{(s,d),(k,z)}[i] = e^{j2\pi i\phi_{(s,z)}} h_{(s,d),(k,z)} x_{(s,d)}[i - \mu_{(s,d)}]$. The expected receive power of node z can be calculated by omitting the items multiplying $\widetilde{v}[i]$ as

$$\begin{aligned}
&\mathbb{E}[|y_{(k,z)}[i]|^2] \\
&= \sum_{(s,d)\in\mathcal{E}} |h_{(s,d),(k,z)}|^2 \mathbb{E}\left[\left|x_{(s,d)}[i - \mu_{(s,d)}]\right|^2\right] \\
&\quad + \sum_{(s,d)\in\mathcal{E}} \sum_{\substack{(l,v)\in\mathcal{E} \\ (l,v)\neq(s,d)}} \mathbb{E}\left[F_{(s,d),(k,z)}[i] F^*_{(l,v),(k,z)}[i]\right] + \sigma_v^2.
\end{aligned}$$

Since $x_{(k,z)}[i]$ and $x_{(s,d)}[i]$ are independent for $(k,z) \neq (s,d)$, we have $\mathbb{E}[x_{(k,z)}[i] x_{(s,d)}[i]^*] = \mathbb{E}[x_{(k,z)}[i]]\mathbb{E}[x_{(s,d)}[i]^*] = 0$, where $\mathbb{E}[x_{(k,z)}[i]] = 0$ for all (k,z)'s, because $x_{(k,z)}[i] = \frac{1}{\sqrt{N}} \sum_{m=0}^{N-1} X_{(k,z)}[m] e^{j2\pi im/N}$ and $\mathbb{E}[X_{(k,z)}[m]] = 0$ for $1 \leq m \leq N$. This implies that when $(k,z) \neq (s,d)$,

$$\begin{aligned}
&\mathbb{E}\left[F_{(s,d),(k,z)}[i] F^*_{(l,v),(k,z)}[i]\right] \\
&= q\mathbb{E}\left[x_{(s,d)}[i - \mu_{(s,d)}]\right] \mathbb{E}\left[x^*_{(l,v)}[i - \mu_{(l,v)}]\right] = 0,
\end{aligned}$$

where $q = h_{(s,d),(k,z)} h^*_{(l,v),(k,z)} \mathbb{E}_{\Delta\phi}\left[e^{j2\pi i\Delta\epsilon}\right]$ and $\Delta\phi = \phi_{(s,z)} - \phi_{(l,z)}$.

References

[1] M. Kamel, W. Hamouda, and A. Youssef, "Ultra-dense networks: A survey," *IEEE Communications surveys & tutorials*, vol. 18, no. 4, pp. 2522–2545, 2016.

[2] B. Yang, G. Mao, M. Ding, X. Ge, and X. Tao, "Dense small cell networks: From noise-limited to dense interference-limited," *IEEE Transactions on Vehicular Technology*, vol. 67, no. 5, pp. 4262–4277, 2018.

[3] Y. Li *et al.*, "A joint scheduling and resource allocation scheme for millimeter wave heterogeneous networks," in *IEEE Wireless Communications and Networking Conference*, 2017.

[4] Z. Ma, B. Li, Z. Yan, and M. Yang, "QoS-Oriented joint optimization of resource allocation and concurrent scheduling in 5G millimeter-wave network," *Computer Networks*, 2020.

[5] Y. Zhao, W. Li, J. Wu, and S. Lu, "A joint scheduling and resource allocation scheme for millimeter wave heterogeneous networks," in *Proc. IEEE INFOCOM*, 2015, pp. 2218–2226.

[6] W. Li, J. Zhang, and Y. Zhao, "Conflict graph embedding for wireless network optimization," in *Proc. IEEE INFOCOM*, 2017, pp. 1–9.

[7] Q. Xue, X. Fang, and C.-X. Wang, "Beamspace SU-MIMO for future millimeter wave wireless communications," *IEEE Journal on Selected Areas in Communications*, vol. 35, no. 7, pp. 1564–1575, 2017.

[8] L. Zhao, D. W. K. Ng, and J. Yuan, "Multi-user precoding and channel estimation for hybrid millimeter wave systems," *IEEE Journal on Selected Areas in Communications*, vol. 35, no. 7, pp. 1576–1590, 2017.

[9] 3GPP, "Study on channel model for frequencies from 0.5 to 100 GHz (Release 16)," TR 38.901, V16.1.0, Dec. 2019.

[10] O. Semiari, W. Saad, M. Bennis, and Z. Dawy, "Inter-operator resource management for millimeter wave multi-hop backhaul networks," *IEEE Transactions on Wireless Communications*, vol. 16, no. 8, pp. 5258–5272, 2017.

[11] W. Cui, K. Shen, and W. Yu, "Spatial deep learning for wireless scheduling," *IEEE Journal on Selected Areas in Communications*, vol. 37, no. 6, pp. 1248–1261, 2019.

[12] M. Lee, G. Yu, and G. Y. Li, "Graph embedding-based wireless link scheduling with few training samples," *IEEE Transactions on Wireless Communications*, vol. 20, no. 4, pp. 2282–2294, 2020.

[13] H. Li, L. Han, R. Duan, and G. M. Garner, "Analysis of the synchronization requirements of 5G and corresponding solutions," *IEEE Communications Standards Magazine*, vol. 1, no. 1, pp. 52–58, 2017.

[14] P. Chen and Z. Yang, "Understanding precision time protocol in today's Wi-Fi networks: A measurement study," in *Proc. USENIX Annual Technical Conference*, 2021, pp. 597–610.

[15] S. Hur, T. Kim, D. J. Love, J. V. Krogmeier, T. A. Thomas, and A. Ghosh, "Millimeter wave beamforming for wireless backhaul and access in small cell networks," *IEEE transactions on communications*, vol. 61, no. 10, pp. 4391–4403, 2013.

[16] A. Ortiz, A. Asadi, G. H. Sim, D. Steinmetzer, and M. Hollick, "Scaros: A Scalable and Robust Self-backhauling Solution for Highly Dynamic Millimeter-wave Networks," *IEEE Journal on Selected Areas in Communications*, vol. 37, no. 12, pp. 2685–2698, 2019.

[17] C. Sun and R. Dai, "Rank-constrained optimization and its applications," *Automatica*, vol. 82, pp. 128–136, 2017.